How to Cite: Petukhov, I.V., Popova, A.M., & Kichigin, V.I. (2023) Electrochemical Processes in Sulfite Gold Plating Solutions and Some Properties of Gold Coatings. *Eurasian Journal of Chemistry, 4(112), 75-81.* https://doi.org/10.31489/2959-0663/4-23-4

Article

Received: 31 May 2023 | Revised: 17 October 2023 |
Accepted: 23 October 2023 | Published online: 15 November 2023

UDC 621.793; 541.138

https://doi.org/10.31489/2959-0663/4-23-4

Igor V. Petukhov[1*], Anna M. Popova[2], Vladimir I. Kichigin[1]

[1]*Perm State University, Perm, Russia;*
[2]*Perm Scientific-Industrial Instrument-Making Company, Perm, Russia*
*(*Corresponding author's e-mail: Petukhov-309@yandex.ru)*

Electrochemical Processes in Sulfite Gold Plating Solutions and Some Properties of Gold Coatings

The kinetics of gold electrodeposition from Au(I) sulfite solutions have been studied by impedance spectroscopy and polarization measurements on a rotating disk electrode. Two solutions were used: a $Na_3Au(SO_3)_2$-based electrolyte with 2,2′-bipyridine as stabilizing additive and an electrolyte containing $(NH_4)_3Au(SO_3)_2$. The polarization curves show a rise in current with increasing rotation speed of the electrode up to 300 rpm. It was found that contributions to the impedance spectra come from the steps of charge transfer and gold adatom incorporation into the crystal lattice, as well as from the relaxation of surface coverage with adsorbed species in an inhibiting layer. An equivalent electrical circuit was suggested to describe the impedance spectra. This circuit provides good approximation of impedance plots for both electrolytes at all electrode potentials. The overall cathodic reaction in both electrolytes appears to consist of the steps of the same nature. Some properties of the Au coatings (micro hardness, size of crystallites) were also determined. Soft gold coatings with micro hardness of 0.66 GPa are obtained from the electrolyte based on $(NH_4)_3Au(SO_3)_2$, the coatings with a higher micro hardness (~0.85 GPa) are deposited from the electrolyte containing 2,2′-bipyridine.

Keywords: gold plating, sulfite electrolyte, 2,2′-bipyridine, ethylenediamine, inhibiting layer, impedance spectroscopy, polarization curve, rotating disk electrode, micro hardness.

Introduction

Sulfite solutions are used for the electrolytic deposition of thick gold coatings in microelectronics, optoelectronics, integrated optics [1–5], for fabricating X-ray gratings [6, 7] and other microstructures [8]. These electrolytes have near-neutral pH value which enables to deposit rather thick (≥ 20 μm) gold layers through photoresist patterns for fabricating different devices operating in microwave band.

From the sulfite electrolytes, bright and soft coatings that have low internal stress even at considerable thickness are obtained [2, 9] if the optimal deposition regime and electrolyte composition were selected. Stabilizing additives are required for stable and long work of sulfite electrolytes.

Another aspect concerning the sulfite gold plating solutions is the need to adjust the bath regularly because sulfite ions are consumed during bath operation at elevated temperature and are oxidized by oxygen in the electrolyte open to the air. For this reason, the electrolytes based on ammonium sulfite have some advantages over the electrolytes based on sodium sulfite since the former are characterized by a much higher concentration of sulfite ions. These circumstances determined the choice of the electrolytes in this work. The aim of this work is to study the effect of sulfite electrolyte composition on the kinetics and mechanism of gold electrodeposition and on some properties of gold coatings.

Experimental

The electrolytic deposition of Au coatings was performed in stirred solutions at a temperature of 50 °C on specimens of copper foil (M0). The copper surface was pre-activated in a 10 % H_2SO_4 solution for 30 s.

Two gold plating electrolytes were studied in this work:

1. Electrolyte No.1 based on sodium sulfite with addition of 2,2′-bipyridine as a stabilizer. The composition is as follows: gold as metal — 8.5 g L^{-1}, sodium sulfite — 40 g L^{-1}, ethylenediamine — 32 g L^{-1}, 2,2′-bipyridine — 0.1 g L^{-1}, pH 7.2. In this electrolyte gold is present as complex compound $Na_3Au(SO_3)_2$. Current density is 20–25 A m^{-2}, current efficiency is 96–98 %.

2. Electrolyte No. 2 based on ammonium sulfite. The composition is as follows: gold as metal — 9.0 g L^{-1}, ammonium sulfite — 100 g L^{-1}, pH 6.8. In this electrolyte gold is present as complex compound $(NH_4)_3Au(SO_3)_2$. Current density is 20–40 A m^{-2}, current efficiency is 94–95 %.

The electrolytes were prepared using deionized water and the following chemicals: sodium sulfite of chemically pure grade, ammonium sulfite monohydrate (Sigma Aldrich), 2,2′-bipyridine of analytical reagent grade, ethylenediamine of analytical reagent grade purified additionally by distillation. Sulfite complexes of gold, $Na_3Au(SO_2)_2$ and $(NH_4)_3Au(SO_3)_2$, were prepared from $HAuCl_4 \cdot H_2O$ (chemically pure) as described in [10].

Electrochemical measurements were carried out on a rotating disk Pt electrode at rotation speeds of 100–300 rpm. To this end a RDE-2 rotating disk electrode unit (Metrohm, Autolab B.V.) was used. Polarization curves were measured in a three-electrode thermostatted cell (at 50 °C) using Autolab potentiostat, model PGSTAT302N. Before measurements, a gold layer of ~1 μm in thickness was deposited on the electrode surface from the electrolyte under study at a current density of 20 A m^{-2} for 8 min. The electrode surface area was 0.07 cm^2. A Pt electrode was used as anode since gold does not dissolve in sulfite electrolytes. The main anodic reaction is the electrooxidation of sulfite ion. All potentials are referred to the NHE scale.

Impedance spectra were measured over a frequency range from 10 kHz to 0.01 Hz at an a.c. signal amplitude of 10 mV using a Solartron 1280Z system. In the course of measurements, the electrode potential was changed in the cathodic direction by steps of 0.02–0.04 V; each potential was held for 10 min to achieve the steady state. Impedance spectra were obtained under the following conditions: 50 °C, rotating electrode, 300 rpm.

The structure of the coatings was studied using scanning electron microscopy (Hitachi S-3400N). The coating micro hardness was measured by the Vickers method using micro hardness tester DM-8 Affri with applied load of 3 g.

Results and Discussion

From the electrolyte No. 1, the coatings were obtained at 2,2′-bipyridine concentration of 0.1 g L^{-1}. When the additive concentration was lower, the stability of electrolyte was insufficient, metallic gold particles appeared in bulk solution; at higher concentrations coatings of poorer quality were obtained: the dendrite growth and coating discontinuities were observed. Addition of 2,2′-bipyridine increased to some extent the coating hardness (up to ~0.85 GPa) and the coating roughness (Fig. 1).

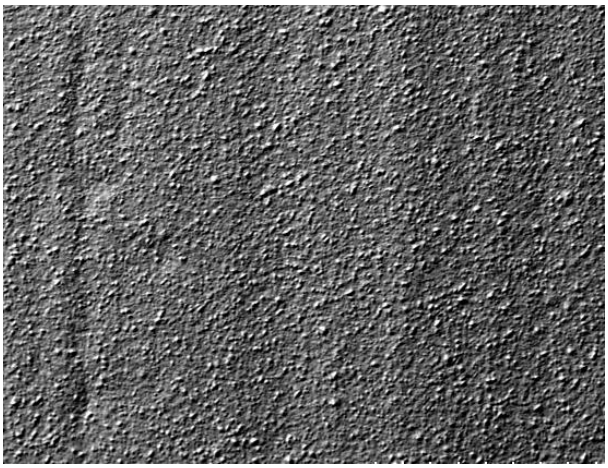

Figure 1. Micrograph of the surface of a coating obtained from the electrolyte No.1. Magnification ×1000

The currents in the electrolyte No.1 increase with rotation speed up to 300 rpm (Fig. 2*a*) while further enhancement of the rotation of the electrode has only slight effect on polarization curve. The polarization curves have three regions of clearly different slope (Fig. 2*a*), with the slope of the first region being 0.08–0.11 V/decade. The adsorption of 2,2′-bipyridine inhibits the electrode process thus resulting in considerably larger magnitudes of cathodic polarization.

From the electrolyte Nao. 2, bright coatings with low hardness (0.66 ± 0.05 GPa) were deposited. To stabilize the electrolyte further, ethylenediamine was added (32 g L^{-1}); this resulted in increasing current efficiency (up to 97–98 %) and micro hardness (up to 0.82 ± 0.04 GPa). As evidenced by electron microscopy, the average size of crystallites decreased from 37 nm to 27 nm (Fig. 3).

The polarization curves in electrolyte No.2 have also a complex shape (Fig. 2*b*). In particular, a larger slope of the polarization curve is observed at moderate current densities. This suggests that an inhibiting layer forms on the electrode surface. At further rise of the polarization, desorption of adsorbed species occurs and the slope decreases again. The electrode rotation has a marked effect only at rather high polarizations, this appears to be related to diffusion limitations in that polarization region. Figure 2 shows typical polarization curves. The relative standard deviation of the current density was about 10–15 %.

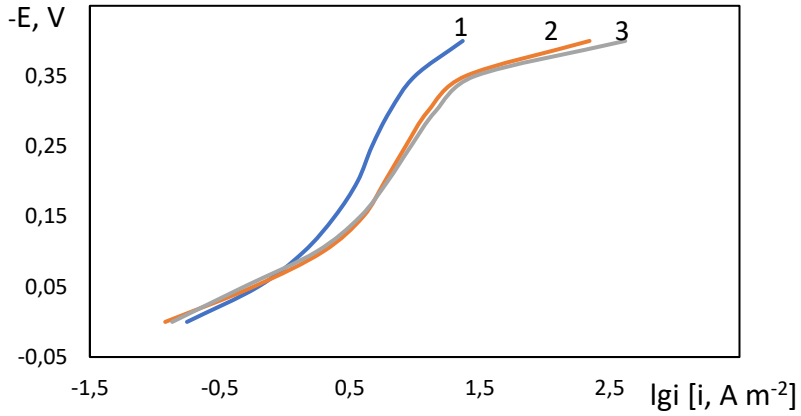

a)

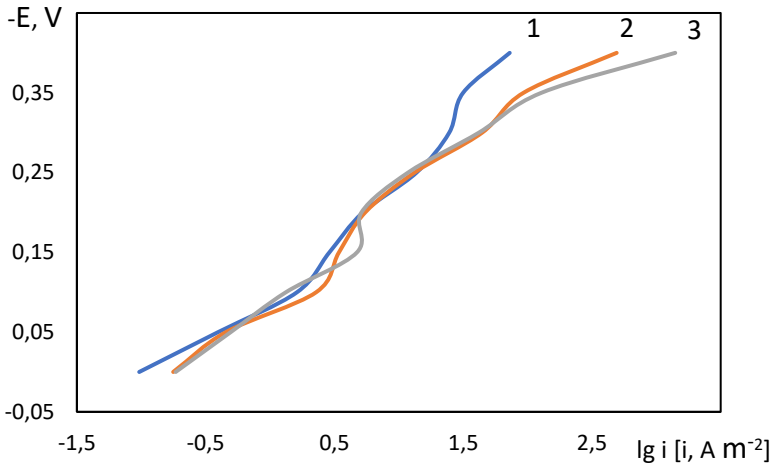

b)

Figure 2. Cathodic polarization curves (*a*) in the electrolyte No. 1 and (*b*) in the electrolyte No. 2 at rotation speeds of 0 (1), 100 (2) and 300 (3) rpm

The overall electrode reaction is:

$$[Au(SO_3)_2]^{3-} + e^- = Au + 2SO_3^{2-}$$

and it can contain several steps (mass transfer, electron transfer, complex ion dissociation, ad-atom incorporation into the crystal lattice) and can be affected by the adsorption of different species. In order to determine the nature of steps in the process under study, the impedance measurements were performed.

For the electrodes on which the gold electrodeposition occurs, two types of the complex plane impedance plots (Fig. 4, 5) were obtained depending on the electrode potential. At low cathodic polarizations, the impedance plot consists of a capacitive arc at high frequencies and an inductive arc at low frequencies (Fig. 4*a*, 5*a*). At higher cathodic polarizations, the impedance plots display two capacitive arcs followed by an inductive arc (Figures 4*b*, 5*b*).

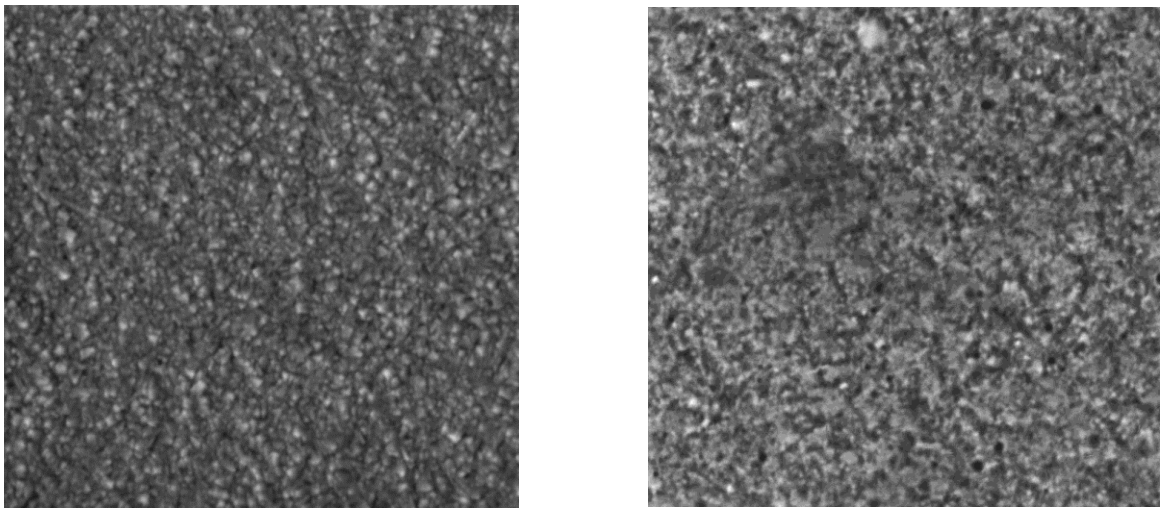

a) *b*)

Figure 3. Micrographs of the surface of coatings obtained from the electrolyte No. 2 (*a*) without ethylenediamine and (*b*) with ethylenediamine additive. Magnification ×100 000

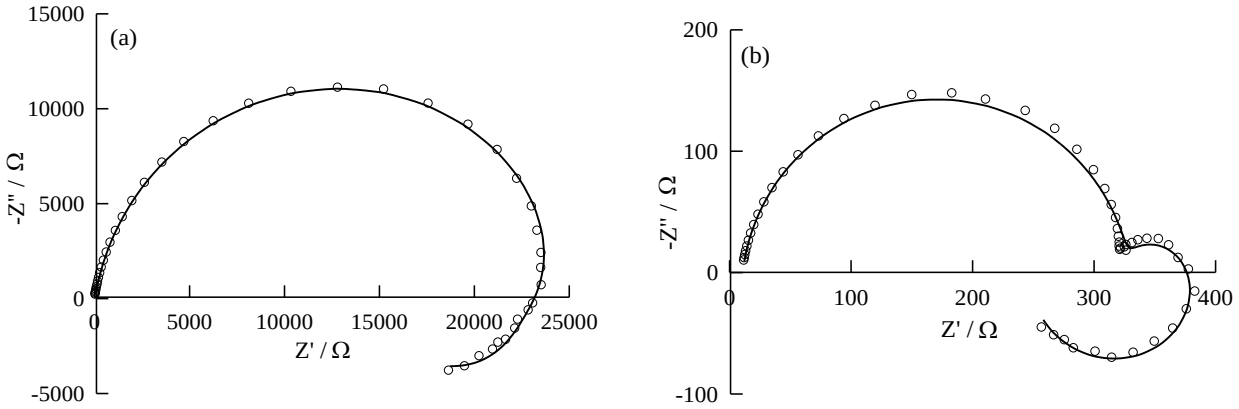

Figure 4. The impedance spectra in electrolyte No. 1. Circles are experimental points, solid lines are fitted curves obtained using the equivalent circuit presented in Figure 6. Electrode potential: (*a*) –0.04 V; (*b*) –0.36 V

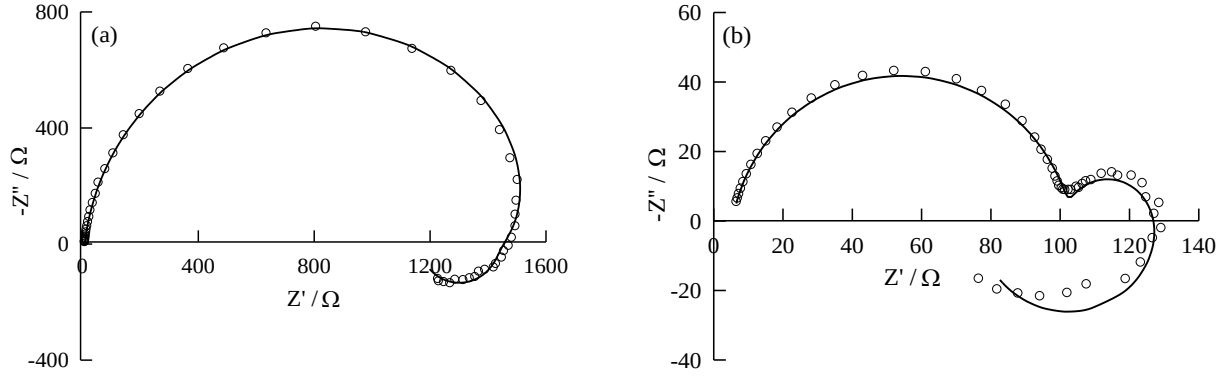

Figure 5. The impedance spectra in electrolyte No. 2. Circles are experimental points, solid lines are fitted curves obtained using the equivalent circuit presented in Figure 6. Electrode potential: (*a*) –0.18 V; (*b*) –0.28 V

The first (high-frequency) capacitive arc corresponds to the charge transfer resistance in parallel with the double layer capacitance. The second capacitive arc is assumed to be related to the incorporation of gold ad-atoms into the crystal lattice. It should be noted that, depending on the conditions, the reagent diffusion in solution can also contribute to the second capacitive arc. However, the impedance was measured at the rota-

tion speed of 300 rpm, when the current, as mentioned above, ceases to change with further increasing rotation speed. Consequently, the diffusion contribution to the impedance is small. The inductive arc can be explained with the following assumptions: additives to the electrolyte adsorb on the electrode surface; adsorption of the additives inhibits the discharge of Au(I) complex ions; adsorption of the additives depends on the electrode potential and decreases as the cathodic polarization increases. The possibility of inductive arc appearing for the charge transfer reaction coupled with inhibitor adsorption has been demonstrated by Mészáros et al. [11].

At gold electrode in sulfite electrolyte, the inhibiting (passivating) layer with which the inductive arc is associated can have a complex composition. The layer supposedly contains chemisorbed sulfite ions and sulfur [12], chemisorbed OH groups, adsorbed molecules of organic compounds (ethylenediamine, bipyridine, etc.). The adsorption in this layer must not be very strong in order that the amount of adsorbate could respond to a sinusoidal potential perturbation used in impedance measurement.

Bipyridine adsorbs well at electrodes from aqueous solutions, and in particular, at Au electrodes from neutral electrolytes [13–16]. The adsorption of 2,2′-bipyridine is potential dependent [14, 15], decreases as the potential is lowered; in a neutral perchlorate solution, desorption of 2,2′-bipyridine from the Au(111) surface is completed at $E \approx$ -0.65 V [14]. Such features of bipyridine adsorption are favorable for an inductive arc to appear in impedance plots.

Taking into account possible steps of the process, an equivalent electrical circuit (Fig. 6) is suggested. The elements of this circuit have the following physical meaning: R_s is the solution resistance, R_1 is the charge transfer resistance, R_2C_2 elements describe the ad-atom incorporation step, and R_3C_3 elements (with negative R and C) are related to the inductive arc. The frequency responses of a negative resistance in parallel with a negative capacitance and of a positive resistance in parallel with a positive inductance are identical at certain relations between the parameter values [17]. Because of this RC couple is also used in the equivalent circuit to model inductive arc. The charge transfer resistance R_1 and R_2C_2 elements (for the ad-atom incorporation step) have the positive sign for the process of metal deposition.

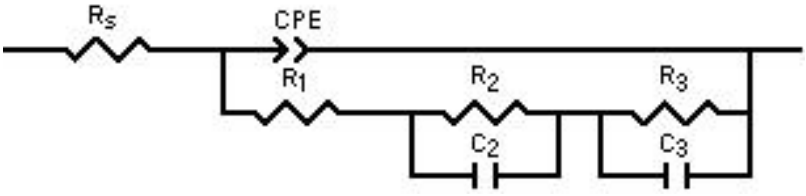

Figure 6. Equivalent electrical circuit

The constant phase element (CPE) is used in equivalent circuit instead of the double layer capacitance. The CPE originates generally from a distribution in the current density along the electrode surface as a result of surface inhomogeneity (geometric, structural, and energetic) [18–20]. The impedance of CPE is $Z_{CPE} = [Q(j\omega)^p]^{-1}$ where j is the imaginary unit, ω is the angular frequency of alternating current, Q is the CPE coefficient, p is the CPE exponent. For gold plating electrolytes studied, p = 0.90–0.91 (electrolyte No. 1) and p = 0.92–0.94 (electrolyte No. 2); the p value depends only slightly on the electrode potential.

The equivalent circuit shown in Figure 6 provides good approximation of both types of impedance spectra (Fig. 4, 5).

At low cathodic polarizations, there is no second capacitive arc (Fig. 4, 5); it can be supposed that the charge transfer is the rate-limiting step under these conditions. The relaxation of the surface coverage in the inhibiting layer is also manifested in this polarization range. When the potential shifts in the negative direction and the charge transfer becomes faster, kinetic limitations arise in the ad-atom incorporation step and the second capacitive arc appears in the impedance plot. The rate-determining step seems still to be the charge transfer as evidenced by the size of two capacitive arcs.

Despite the variations in electrolyte composition, the impedance plots are similar (Fig. 4, 5) and the experimental impedance spectra can be fitted using the same equivalent circuit for both electrolytes. Thus, the steps comprising the mechanism for the overall cathodic reaction are of the same nature in electrolyte No.1 and No.2. Some differences between the impedance spectra in the investigated electrolytes are mainly due to the variations in the values of rate constants of the steps and in the properties of inhibiting layers on the electrode surface.

Conclusions

The kinetics and mechanism of gold electrodeposition were studied in two sulfite electrolytes: (i) an electrolyte containing $Na_3Au(SO_3)_2$ and 2,2′-bipyridine additive; (ii) an electrolyte containing $(NH_4)_3Au(SO_3)_2$. Bipyridine adsorbs well at Au electrode, inhibits the electrode process and has an appreciable effect on the properties of Au coatings. In particular, addition of 2,2′-bipyridine increases the coating hardness up to ~0.85 GPa. From the electrolyte based on ammonium sulfite, the coatings with a lower hardness (0.66 ± 0.05 GPa) are deposited.

The impedance spectroscopy data suggest that the overall cathodic process in both electrolytes involves the steps of charge transfer and gold ad-atom incorporation into the crystal lattice; the relaxation of surface coverage with adsorbed species also affects the impedance spectra.

Acknowledgements

The research was supported by the Perm Scientific and Educational Center “Rational Subsoil Use”, 2023.

References

1 Osaka, T., Okinaka, Y., Sasano J., & Kato, M. (2006). Development of new electrolytic and electroless gold plating processes for electronics applications. *Science and Technology of Advanced Materials*, 7, 425–437. https://doi.org/10.1016/j.stam.2006.05.003

2 Green, T.A. (2007). Gold electrodeposition for microelectronic, optpelectronic and microsystem applications. *Gold Bulletin*, *40* (2), 105–114. https://doi.org/10.1007/BF03215566

3 Dimitrijević, S., Rajčić-Vujasinović, M., & Trujić, V. (2013). Non-cyanide electrolytes for gold plating — a review. *Int. J. Electrochem. Sci.*, 8, 6620–6646.

4 Josell, D., & Moffat, T. P. (2019). Bottom-up filling of damascene trenches with gold in a sulfite electrolyte. *J. Electrochem. Soc.*, 166, D3022–D3034. https://doi.org/10.1149/2.0041901jes

5 Lintao Liu, Xiaoli Zhu, Shuhua Wei, Jing Zhang, M.R. Baklanov, A.B. da Silva Fanta, Jiebin Niu, & Changqing Xie. (2019). Influence of current density on orientation-controllable growth and characteristics of electrochemically deposited Au films. *J. Electrochem. Soc.* 166, D3232–D3237. https://doi.org/10.1149/2.0291901jes

6 Josell, D., & Moffat, T.P. (2023). Extreme bottom-up gold filling of high aspect ratio features. *Acc. Chem. Res. 56*(6), 677–688. https://doi.org/10.1021/acs.accounts.2c00826

7 Ohlin, H., Frisk, T., Åstrand, M., & Vogt, U. (2022). Miniaturized sulfite-based gold bath for controlled electroplating of zone plate nanostructures. *Micromachines 13*(3), 452. https://doi.org/10.3390/mi13030452

8 Schürch, P., Osenberg, D., Testa, P., Bürki, G., Schwiedrzik, J., Michler, J., & Koelmans, W.W. (2023). Direct 3D microprinting of highly conductive gold structures via localized electrodeposition. *Materials & Design*, 227, 111780. https://doi.org/10.1016/j.matdes.2023.111780

9 Kichigin, V.I., Petukhov, I.V., Shevtsov, D.I., & Permyakova M.A. (2015). Electrodeposition of coatings from sulfite gold-plating electrolyte and their properties. *Russ. J. Appl. Chem.*, 88, 1950–1957. https://doi.org/10.1134/S10704272150120083

10 Karyakin, Yu.V., & Angelov, I.I. (1974). *Chistye Khimicheskie Veshchestva [Pure Chemical Substances]*. Moscow: Khimiia [in Russian].

11 Mészáros, L., Lengyel, B., & Garai, T. (1982). Study of inhibitors by electrode impedance measurements. *Acta Chim. Acad. Sci. Hung.*, 110, 57–65.

12 Baltrūnas, G., Valiūnienė, A., Vienožinskis, J., Gaidamauskas, E., Jankauskas, T., & Margarian, Ž. (2008). Electrochemical gold deposition from sulfite solution: application for subsequent polyaniline layer formation. *J. Appl. Electrochem.*, 38, 1519–1526. https://doi.org/10.1007/s10800-008-9596-1

13 Mambetkaziev, E.A., Zhdanov, S.I., & Damaskin, B.B. (1972). Uchet vliianiia adsorbtsii ligandov i kompleksov pri issledovanii kompleksoobrazovaniia poliarograficheskim metodom. I. Issledovanie adsorbtsii 2,2′-dipiridila na rtuti iz vodnykh rastvorov KNO_3 [Account of the adsorption of ligands and complexes in complexation study by polarographic method. I. A study of 2,2′-bipyridine adsorption on mercury from aqueous KNO_3 solutions]. *Elektrokhimiia — Electrochemistry*, *8*(11), 1650–1654 [in Russian].

14 Dretschke, Th., & Wandlowski, Th. (1999). An order-disorder-order adlayer transition of 2,2′-bipyridine on Au(III). *Electrochim. Acta*, 45, 731–740. https://doi.org/10.1016/S0013-4686(99)00252-2

15 Zeng, X., & Hatton, R. (2000). EQCM study of adsorption of bipyridine on Au polycrystalline electrode using underpotential deposition of Pb as a probe. *Electrochim. Acta*, 45, 3629–3638. https://doi.org/10.1016/S0013-4686(00)00446-1

16 Ren, X., Song, Y., Liu, A., Zhang, J., Yuan, G., Yang, P., et al. (2015). Computational chemistry and electrochemical studies of adsorption behavior of organic additives during gold deposition in cyanide-free electrolytes. *Electrochim. Acta*, 176, 10–17. https://doi.org/10.1016/j.electacta.2015.06.147

17 Lasia, A. (2014). Electrochemical Impedance Spectroscopy and its Applications. Springer Science + Business Media, New York.

18 Córdoba-Torres, P., Mesquita, T.J., & Nogueira, R.P. (2015). On the relationship between the origin of constant-phase element behavior in electrochemical impedance spectroscopy and electrode surface structure. *J. Phys. Chem. C*., 119(8), 4136–4147. https://doi.org/10.1021/jp512063f

19 Alexander, C.L., Tribollet, B., & Orazem, M.E. (2015). Contribution of surface distributions to constant-phase-element (CPE) behavior: 1. Influence of roughness. *Electrochim. Acta*, 173, 416–424. https://doi.org/10.1016/j.electacta.2015.05.010

20 Pajkossy, T., & Jurczakowski, R. (2017). Electrochemical impedance spectroscopy in interfacial studies. *Current Opinion in Electrochemistry*, 1, 53–58. https://doi.org/10.1016/j.coelec.2017.01.006

Information about authors*

Petukhov, Igor Valentinovich (*corresponding author*) — Candidate of chemical sciences, Associate Professor, Perm State University, Bukireva st., 15,, 614097, Perm, Russia; e-mail: Petukhov-309@yandex.ru, https://orcid.org/0000-0002-3110-668x

Popova, Anna Mikhailovna — Head of the Laboratory, Perm Scientific-Industrial Instrument-Making Company, 25th October st., 106, 614007, Perm, Russia; e-mail: AMPopova@pnppk.ru

Kichigin, Vladimir Ivanovich — Candidate of chemical sciences, Senior Researcher, Perm State University, Bukireva st., 15, 614097, Perm, Russia; e-mail: kichigin@psu.ru, https://orcid.org/0000-0002-4668-0756

*The author's name is presented in the order: *Last Name, First and Middle Names*